Accepted Manuscript

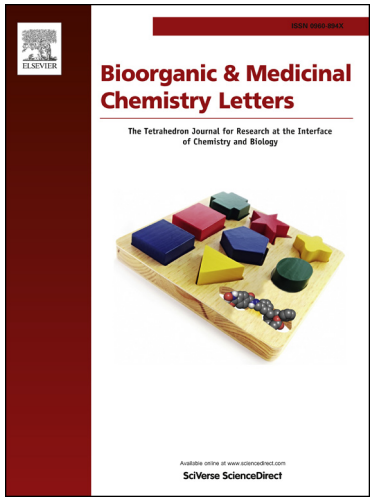

Discovery and structural diversity of the hepatitis C virus NS3/4A serine protease inhibitor series leading to clinical candidate IDX320

Christophe C. Parsy, François-René Alexandre, Valérie Bidau, Florence Bonnaterre, Guillaume Brandt, Catherine Caillet, Sylvie Cappelle, Dominique Chaves, Thierry Convard, Michel Derock, Damien Gloux, Yann Griffon, Lisa B. Lallos, Frederic Leroy, Michel Liuzzi, Anna-Giulia Loi, Laure Moulat, Musiu Chiara, Virginie Roques, Elodie Rosinovsky, Simon Savin, Maria Seifer, David Standring, Dominique Surleraux

PII: S0960-894X(15)30041-X
DOI: http://dx.doi.org/10.1016/j.bmcl.2015.09.009
Reference: BMCL 23090

To appear in: *Bioorganic & Medicinal Chemistry Letters*

Received Date: 1 June 2015
Revised Date: 2 September 2015
Accepted Date: 4 September 2015

Please cite this article as: Parsy, C.C., Alexandre, o-R., Bidau, V., Bonnaterre, F., Brandt, G., Caillet, C., Cappelle, S., Chaves, D., Convard, T., Derock, M., Gloux, D., Griffon, Y., Lallos, L.B., Leroy, F., Liuzzi, M., Loi, A-G., Moulat, L., Chiara, M., Roques, V., Rosinovsky, E., Savin, S., Seifer, M., Standring, D., Surleraux, D., Discovery and structural diversity of the hepatitis C virus NS3/4A serine protease inhibitor series leading to clinical candidate IDX320, *Bioorganic & Medicinal Chemistry Letters* (2015), doi: http://dx.doi.org/10.1016/j.bmcl.2015.09.009

This is a PDF file of an unedited manuscript that has been accepted for publication. As a service to our customers we are providing this early version of the manuscript. The manuscript will undergo copyediting, typesetting, and review of the resulting proof before it is published in its final form. Please note that during the production process errors may be discovered which could affect the content, and all legal disclaimers that apply to the journal pertain.

ACCEPTED MANUSCRIPT

Graphical Abstract

To create your abstract, type over the instructions in the template box below.
Fonts or abstract dimensions should not be changed or altered.

Discovery and structural diversity of the hepatitis C virus NS3/4A serine protease inhibitor series leading to clinical candidate IDX320

Leave this area blank for abstract info.

Christophe C. Parsy[a, *], François-René Alexandre[a], Valérie Bidau[a#], Florence Bonnaterre[a#], Guillaume Brandt[a], Catherine Caillet[a#], Sylvie Cappelle[a], Dominique Chaves[a#], Thierry Convard[a], Michel Derock[a#], Damien Gloux[a#], Yann Griffon[a#], Lisa B. Lallos[b#], Frederic Leroy[a#], Michel Liuzzi[b#], Anna-Giulia Loi[b#], Laure Moulat[a#], Musiu Chiara[b#], Virginie Roques[a#], Elodie Rosinovsky[a#], Simon Savin [a#], Maria Seifer[b], David Standring[b#] and Dominique Surleraux[a#]

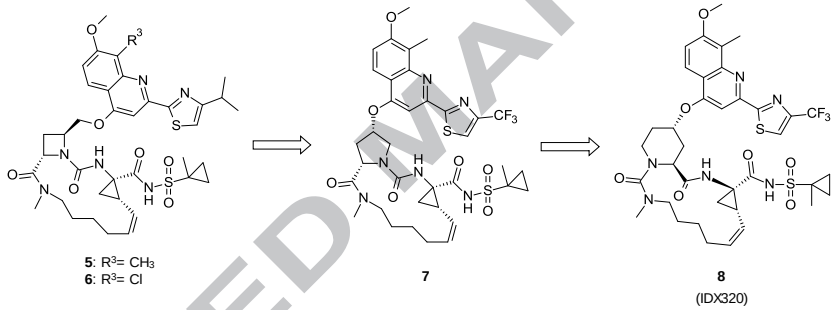

ACCEPTED MANUSCRIPT

ACCEPTED MANUSCRIPT

Bioorganic & Medicinal Chemistry Letters
journal homepage: www.elsevier.com

Discovery and structural diversity of the hepatitis C virus NS3/4A serine protease inhibitor series leading to clinical candidate IDX320

Christophe C. Parsy[a, *], François-René Alexandre[a], Valérie Bidau[a#], Florence Bonnaterre[a#], Guillaume Brandt[a], Catherine Caillet[a#], Sylvie Cappelle[a], Dominique Chaves[a#], Thierry Convard[a], Michel Derock[a#], Damien Gloux[a#], Yann Griffon[a#], Lisa B. Lallos[b#], Frederic Leroy[a#], Michel Liuzzi[b#], Anna-Giulia Loi[b#], Laure Moulat[a#], Musiu Chiara[b#], Virginie Roques[a#], Elodie Rosinovsky[a#], Simon Savin[a#], Maria Seifer[b], David Standring[b#] and Dominique Surleraux[a#]

[a]*IDENIX*, a wholly-owned subsidiary of Merck & Co, *1682 rue de la Valsière, Cap Gamma, BP 50001, 34189 MONTPELLIER Cedex 4, FRANCE*
[b]*IDENIX*, a wholly-owned subsidiary of Merck & Co, *320 Bent Street - 4th Floor, Cambridge, MA 02139, USA*
[#]*Former Idenix employees*

ARTICLE INFO

Article history:
Received
Revised
Accepted
Available online

Keywords:
Hepatitis C
HCV NS3/4A protease inhibitors
Macrocycle

ABSTRACT

Exploration of the P2 region by mimicking the proline motif found in BILN2061 resulted in the discovery of two series of potent HCV NS3/4a protease inhibitors. X-Ray crystal structure of the ligand in contact with the NS3/4A protein and modulation of the quinoline heterocyclic region by structure based design and modeling allowed for the optimization of enzyme potency and cellular activity. This research led to the selection of clinical candidate IDX320 having good genotype coverage and pharmacokinetic properties in various species.

2015 Elsevier Ltd. All rights reserved.

Current reports indicate that 3% of the world's population is infected with Hepatitis C virus (HCV), which leads to chronic hepatitis. In some cases, this progress to liver cirrhosis and hepatocellular carcinoma; HCV is the main cause of liver transplantation in developed countries.[1] The previous standard of care introduced in 2001 covering all HCV genotypes, combining pegylated interferon and ribavirin, induces a sustained viral response (SVR) in about 50% of patients affected by HCV genotype 1, highlighting the need for more effective chemotherapeutic agents to treat HCV patients.[2] Recent advances in treatment options with the approval of sofosbuvir (nucleoside polymerase inhibitor) and the combination of sofosbuvir and ledipasvir (NS5A replication inhibitor) has seen dramatic cure rate up to 99% in some specific genotype population patients.[3] It is likely that the next evolution in HCV therapy will be the identification of a pan-genotypic direct acting antiviral combination therapy including an NS3/4A protease inhibitor that could shorten the treatment duration below the current 12 weeks across all HCV patient population.

The understanding of the HCV genomic organization, life cycle of the virus, as well as the development of HCV replicons has enhanced rational drug design efforts and led to the discovery of direct acting antiviral inhibitors of HCV protease.[4–7] Currently, two classes of protease inhibitors have emerged (Chart 1). The serine trap inhibitors, such as telaprevir[8] (VX-950) (**1**) and boceprevir[9] (SCH-503034) (**2**), include the first class and are constructed around an α-ketoamide moiety that covalently and reversibly binds S139, part of the catalytic triad of the HCV protease. Due to the recent progress in HCV treatment option, (**1**) and (**2**) are no longer recommended for regimen therapy and discontinued.[10] The second class resulted from the discovery that the N-terminal cleavage product from the NS5A/B cleavage site is a competitive inhibitor of the NS3 protease. Truncation of this hexapeptide to a tetrapeptide on a rigid macrocyclic scaffold yielded the non-covalent macrocyclic protease inhibitor, BILN 2061 (**3**). This was the first HCV protease inhibitor to enter clinical trials, and in only 2 days of monotherapy reduced viral RNA by 2-3 $\log_{10}$ IU/mL in patients, thereby establishing

* Corresponding author. Tel.: +33(0)499522252; fax: +33(0)499522250; e-mail: christophe.parsy@merck.com

ACCEPTED MANUSCRIPT

proof of concept for HCV protease as a viable antiviral target.[11–14] Unfortunately, BILN-2061 had to be discontinued due to cardiac toxicities in animal studies.[15] Despite the fact that the mechanism of cardiac toxicity has not been reported, it is believed to be compound specific and several groups, inspired by this pioneer drug, have pursued macrocyclic inhibitors leading to the approval of simeprevir (**4**).[16]

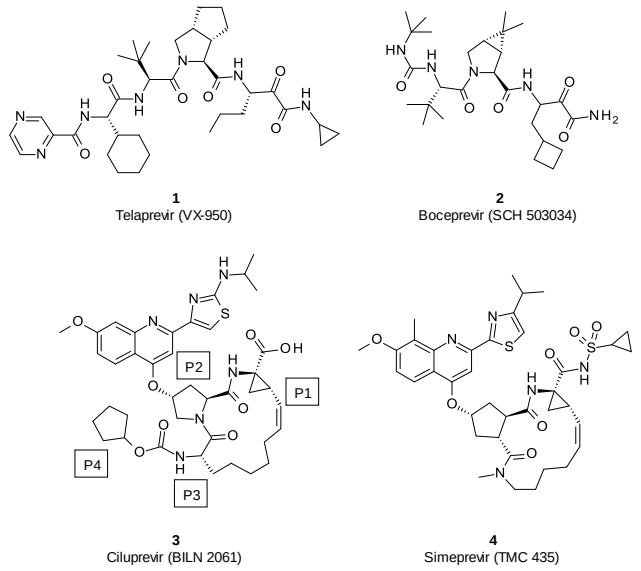

Chart 1. First generation of NS3/4A protein inhibitors

In this letter, we present our continuous efforts originated from the 2,4-disubstituted azetidine motif (**5**) and (**6**) in the P2 region.[17] We designed two novel series of macrocyclic HCV protease inhibitors by introducing structure diversity at the P2 region (Chart 2). The first series differs from BILN2061 by switching position 1 and 2 of the proline ring therefore creating a proline urea moiety (**7**). The second series represents a ring expansion of P2 region by using pipecolic acid instead of pyrrolidine acid as a starting building block. These efforts led to the clinical drug candidate IDX320 (**8**).

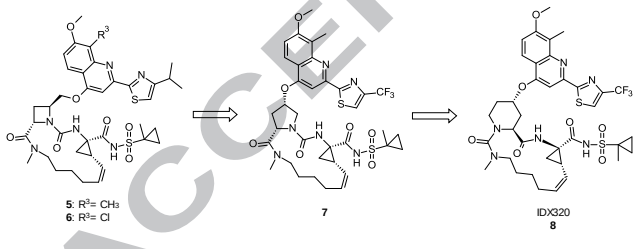

Chart 2. From a lead series to the drug candidate IDX320

The synthesis of the proline urea series was based on a 4-hydroxy proline scaffold and started from the commercially available N-Boc protected 4-hydroxy-2-pyrrolidine carboxylic acid (**9**) (Scheme 1). Peptide coupling with the N-methyl hexenyl mediated by TBTU, Boc-deprotection, coupling with the 1,1'-carbonyldiimidazole (CDI) activated vinylcyclopropyl amino acid ester followed by protection of the pyrrolidine hydroxyl by *tert*-butyldimethylsilyl chloride (TBDMSCl) or 4-nitrobenzoyl chloride resulted in the diene (**11**). This diene (**11**) was then engaged in a Ruthenium catalysed ring closing metathesis (RCM) followed by deprotection of the hydroxyl group to yield the 14-membered macrocycle (**12**).[18] The RCM can be carried out with Hoveyda-Grubs[19] 1st or 2nd generation catalyst or Zhan's catalyst[20] along with DarPhin catalyst developed in our laboratories.[21] This synthetic strategy enabled us to introduce diversity on the macrocycle using different quinoline rings (**13a-w**) with a straightforward Mitsunobu coupling. After coupling of the quinoline and hydrolysis of the ester, the resulting acid (**15**) was activated by CDI to form an intermediate oxazolidinedione that is open in the presence of the P1 sulfonamide to yield the final target inhibitors (**16a-x**) and (**7**).

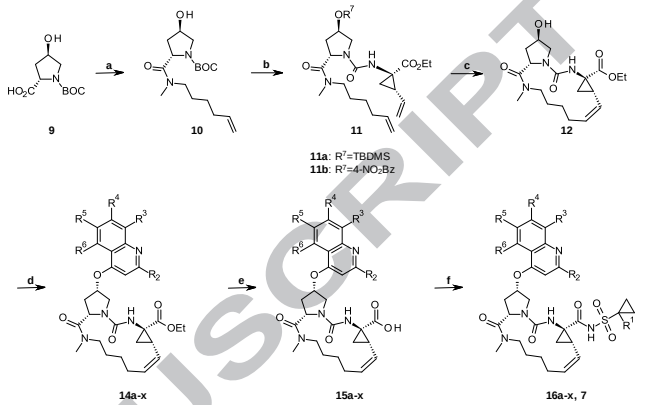

Scheme 1. Reagents and conditions: (a) TBTU, diisopropylethylamine, N-methylhex-5-en-1-amine tosylate salt, DMF, 0°C to RT, 16h, 95%; (b) (1) TFA, DCM, RT, 3h, quant. (2) ethyl (1*R*,2*S*)-1-[(3-methylimidazol-3-ium-1-carbonyl)amino]-2-vinyl-cyclopropanecarboxylate, Et_3N, DCM, RT, 16h, 70%, (3i) TBDMSCl, Et_3N, DCM, RT, 16h, 70% or (3ii) 4-nitrobenzoyl chloride, Et_3N, DCM, RT, 16h, 46-70%; (c) (1) Hoveyda-Grubbs 2nd generation cat. or Zhan II cat., DCE reflux, 3h, 43-64%, (2i) TBAF, THF, RT, 2h, 94% or (2ii) LiOH, H_2O/THF, 0°C, 45min, 71-81%; (d) quinolines **13a-w**, PPh_3, DIAD, THF, 0°C to RT, 16h, 15-89%; (e) LiOH, H_2O/THF, RT, 16h, 10-90%; (f) (1) CDI, THF or EDCI, DCM, 80°C, microwaves irradiations, 50min, (2) DBU, 1-methylcyclopropylsulfonamide or cyclopropylsulfonamide, 80°C, microwaves irradiations, 1h30, 9-51%.

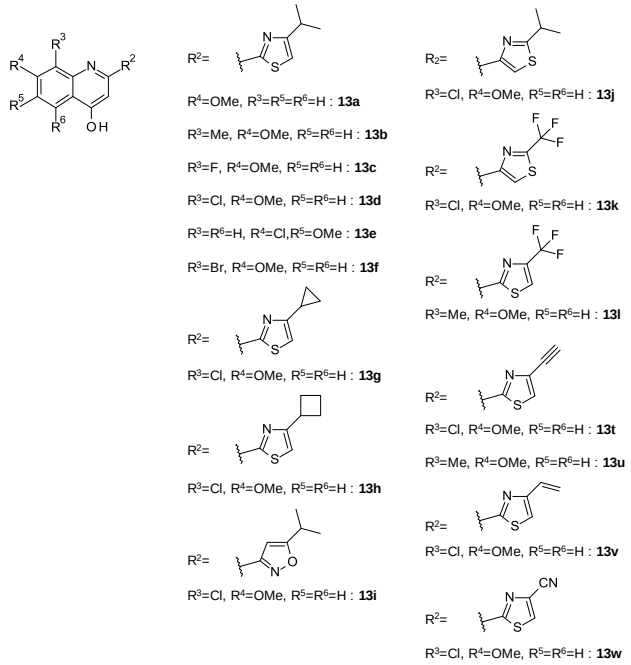

Chart 3. Quinolines (**13a-l**), (**13t-w**).

2-Thiazoles, 4-thiazoles, 3-oxazoles and 2-oxazoles substituted quinolines (**13a-l**) and (**13t-w**) (Chart 3) were synthesised using described methods, starting from ortho-acyl anilines and corresponding thiazole or oxazole acids.[16,22] It should be noted that for (**13t-w**), functionalizations (Sonogashira and Heck reactions) at the position 4 of the 4-bromo-thiazole were realized before the cyclisation step,

ACCEPTED MANUSCRIPT

unless no reaction was observed. Quinolines (**13m-s**) were prepared according to scheme 2 using a concise synthesis in four or five steps from anilines (**17a-b**). First step consisted in a cyclisation reaction of malonic acid in the presence of phosphorus oxychloride to yield the 2,4-dichloroquinolines (**18a-b**). Then the 4 position was protected in 50% yield with the reaction of para-methoxybenzyl alcohol (PMB) giving a mixture of major 4-OPMB and minor 2-OPMB adducts, which were easily separable by chromatography on silica gel. N-branched pyrazoles were then introduced *via* a SNAr reaction in moderate yields, followed by PMB deprotection using TFA to afford (**13m-n**). (**13p-r**) were obtained *via* Negishi, Suzuki-Miyaura, or Stille reaction at position 2, followed by TFA treatment. Triazole (**13o**) was synthesised from 2-azido quinoline (**20b**) followed by cyclisation with ethynyl derivatives. Oxadiazole (**13s**) was obtained from 2-cyano-quinoline (**20a**) then reaction with hydroxylamine and followed by cyclisation with isobutyryl chloride.

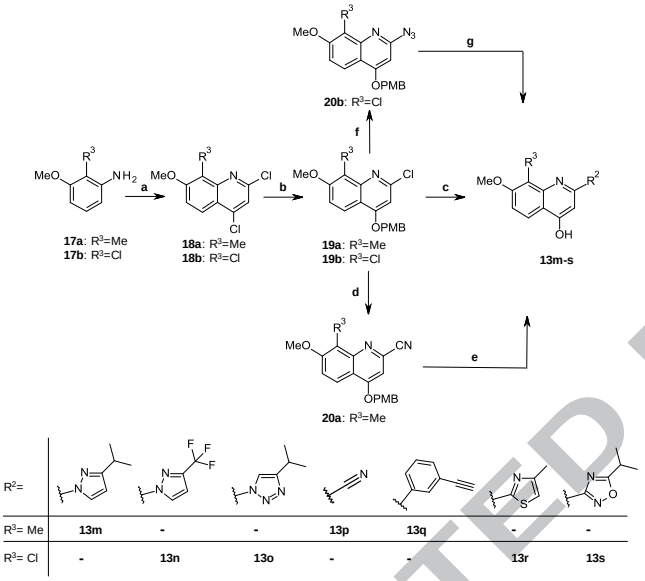

Scheme 2. Reagents and conditions: (a) malonic acid, $POCl_3$, reflux, 16h, 63-75% ; (b) *p*-methoxybenzylalcohol, NaH, 15-crown-5, DMF, 0°C to RT, 16h, 50-72%; (c) (i) pyrazole, NMP, 200°C, microwaves irradiations, 30min, 33%, for **13m**; or (ii) (1) pyrazole, NaH, DMF, 0°C to 90°C, 6h, 50%; (2) $CeCl_3.7H_2O$, NaI, CH_3CN, 85°C, microwaves irradiations, 1h, 58%; for **13n**; or (iii) (1) (3-(2-trimethylsilylethynyl) phenyl) boronic acid, $Pd(OAc)_2$, PPh_3, Na_2CO_3, H_2O, dioxane, 100°C, microwaves irradiations, 1h, 52%; (2) TFA, RT, 10min, quant.; for **13q**; or (iv) (1) 4-methyl-2-(tributylstannyl)thiazole, $PdCl_2(PPh_3)_2$, K_2CO_3, DMF, 90°C, 16h, 65%; (2) TFA, RT, 10min, quant.; for **13r**; (d) Zn, $Zn(CN)_2$, Pd_2dba_3, dppf, DMA, 120°C, microwaves irradiations, 70min, 67%; (e) (i) TFA, RT, 10min, 92% for **13p**; or (ii) (1) $NH_2OH.HCl$, TEA, EtOH, reflux, 3h30; (2) isobutyryl chloride, isobutyric acid, 100°C, 3h, 87%; for **13s**; (f) NaN_3, DMF, 80°C, 48h, 12%; (g) (1) 3-methylbutyne, CuI, DIPEA, DMF, 140°C, microwaves irradiations, 45min, 84%; (2) TFA, DCM, RT, 10min, 94%; for **13o**.

The pipecolic series was based on a 4-hydroxy pipecolic scaffold. Two different synthetic routes were used for this scaffold. The first strategy was similar to the previously described in Scheme 1 for the 4-hydroxy proline scaffold and was used to synthesize compound (**27**) (Scheme 3). The second route involved coupling the quinoline motif as the first step of the synthesis then building-up the macrocycle stepwise to finish using the ring closing metathesis reaction to yield the final inhibitor. This route was less convergent but represented a possible strategy that could be used in a scale-up process. This synthetic route has been successfully used for the synthesis of compound (**31a**) and (**8**) (Scheme 4).

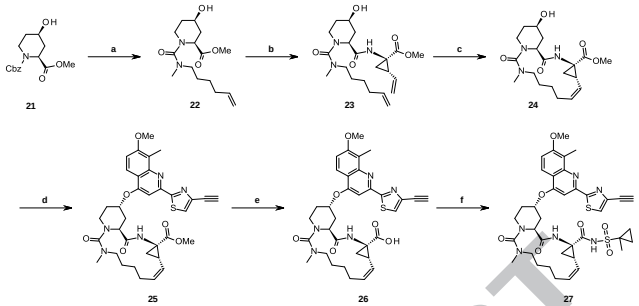

Scheme 3. Reagents and conditions: (a) (1) H_2, Pd/C, EtOH, RT, 16h, quant., (2) Et_3N, N-hex-5-enyl-N,3-dimethyl-imidazol-3-ium-1-carboxamide iodide, THF, 120°C, microwaves irradiations, 1h, 66%; (b) (1) LiOH, H_2O/THF, RT, quant., 16h, (2) TBDMSCl, Imidazole, DMF, RT, 20h, 76%, (3) [(1R,2S)-1-methoxy-carbonyl-2-vinyl-cyclopropyl]ammonium tosylate salt, DIPEA, TBTU, DCM, RT, 16h, 48%; (c) Hoveyda-Grubbs 1st generation cat., DCE reflux, 4h, 54%; (d) **13u**, PS-PPh_3, DIAD, THF, 0°C to RT, 16h, 42%; (e) LiOH, H_2O/THF, RT, 16h, 46%; (f) (1) EDCI, DCM, RT, 3h, (2) DBU, 1-methylcyclopropylsulfonamide, RT, 3h, 50%.

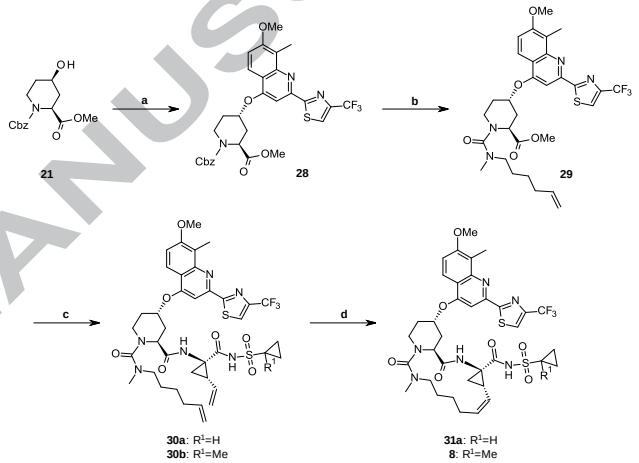

Scheme 4. Reagents and conditions: (a) **13l**, PPh_3, DIAD, THF, 0°C to RT, 2h, 52%; (b) (1) TFA, 60°C, 5h, 97%, (2) Et_3N, N-hex-5-enyl-N,3-dimethyl-imidazol-3-ium-1-carboxamide iodide, THF, 120°C, microwaves irradiations, 1h, 78%; (c) (1) LiOH, H_2O/THF, 40°C, 16h, 90%, (2) (1*R*,2*S*)-1-amino-N-cyclopropyl-sulfonyl-2-vinyl-cyclopropane-carboxamide or (1*R*,2*S*)-1-amino-N-(1-methylcyclopropyl)sulfonyl-2-vinyl-cyclopropanecarboxamide, DIPEA, TBTU, DMF, RT, 16h, 30-93%; (d) Zhan IB cat., DCE reflux, 1h, 20-36%.

Our previous research efforts on the discovery of HCV protease inhibitors led to a novel series of β-strand mimic having 2,4-disubstituted azetidine motif in the P2 region.[17] The best compounds from this series (**5**) and (**6**) (Chart 2) demonstrated excellent biochemical activity IC_{50} 6.6 and 2.1 nM and good inhibition of HCV replicon replication in Huh-7 cells containing Con1 subgenomic replicon (GS4.1 cells) monitored for expression of the NS5A protein with EC_{50} = 45 and 60 nM, respectively, and good selectivity indices (SI) >1500. Further *in vitro* evaluation of these two compounds demonstrated high mean clearance (>150 µl/min/mg prot) in rat, cynomolgus monkey and human liver microsomes, along with a short half life (<10 minutes) confirmed by *in vivo* studies in the rat (Table 3). Anticipating a possible sensitivity of the azetidine ring toward metabolic degradation, this series was no longer pursued.

We investigated the 3-hydroxy-pyrrolidine as a possible mimic keeping the urea motif within the macrocycle. Molecular modeling of this series indicated that canonical hydrogen bonds between the amide moieties of the inhibitor and the NS3 main chain would be maintained. The first compound synthesized bore an 8-fluorine on the quinoline moiety, compound (**16c**). The compound exhibited excellent biochemical activity (IC_{50}=3.5 nM) but moderate inhibitory

ACCEPTED MANUSCRIPT

activity in a luciferase-replicon cell based assay (EC_{50}=538 nM) (Table 1).

Compound (**16c**) was selected for co-crystallization with the NS3/4A protein and rapidly yielded suitable crystals. The structure was solved and refined to a final resolution of 2.8 Å in which the stereochemistry of all chiral centers was confirmed.[23] Examination of the crysta1 structure revealed that the protease active site is extremely hydrophobic and flat whereas the catalytic center is relatively exposed to solvent. Nevertheless, ligand (**16c**) forms six specific hydrogen bonds with the protein (Figures 1 and 2): four main chain interactions (G137, S139, A157 and R155) and two side chain interactions (K136 and S139). It is also possible to observe a sigma-π interaction between H57 and one of the proline C5-hydrogen on the ligand.[24,25]

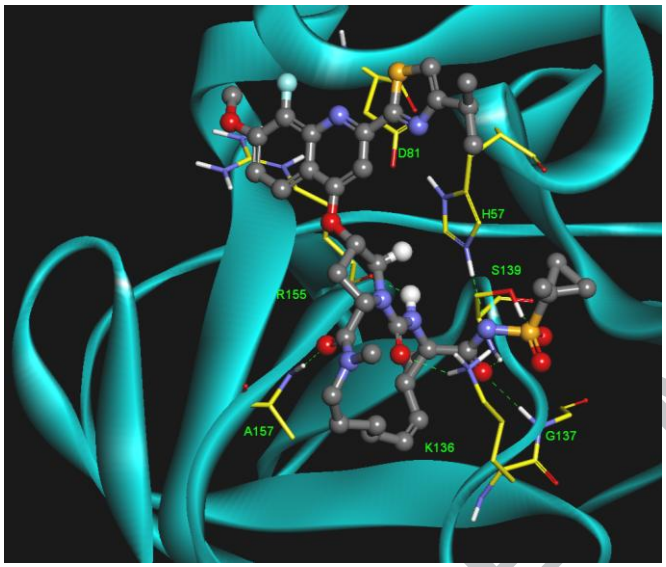

Figure 1. Representation of the amino acids of NS3/4A protein directly involved in main chain or side chain interactions with compound (**16c)** in the catalytic centre of the HCV protease. (PDB code: 4U01)

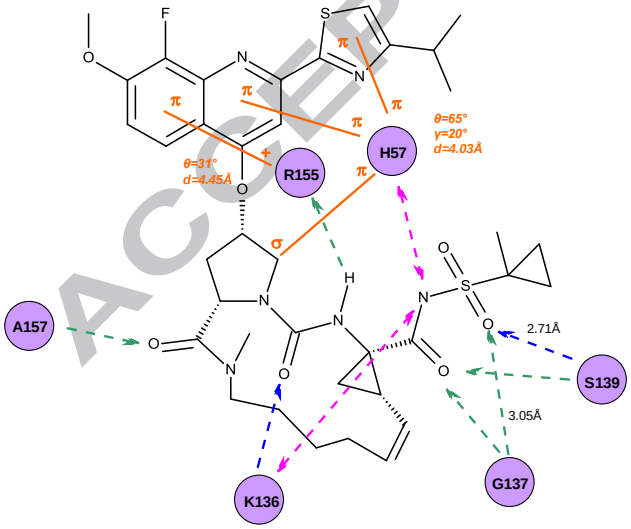

Figure 2. 2D-cartography of the interactions observed between compound (**16c**) and the NS3/4A protein.
Green doted arrow: Main chain hydrogen bond interactions; Blue doted arrow: Side chain hydrogen bond interactions; Magenta doted arrow: Charge interactions; Orange Line: π interactions

Rönn et al[26] emphasized the importance of both sulfonyl oxygens for excellent enzymatic and cell based potencies. It can be seen from this crystal structure that one of the sulfonamide oxygen atoms is involved in the hydrogen bonding interaction with G137 and S139 in the oxyanion hole of the serine protease. In this example, the adjacent carbonyl is also involved in hydrogen bonding with G137 and S139 main chain thereby forming a strong hydrogen bond network. A remarkable difference between our modeling and the crystal structure is the orientation of K136; the alkyl side chain is overlapping the macrocycle with the terminal amine making a hydrogen bond interaction with the urea carbonyl. K136 is acting like a claw forming a well defined pocket with the oxyanion hole and the catalytic triad in which the macrocyclic moiety of the inhibitor is making strong main chain and side chain interactions. Having such an intricate network of interactions on the macrocyclic moiety, we decided to turn our attention to the quinoline heterocyclic region. The quinoline motif is parallel and above the axis formed by the δ-NH of H57 and the COO^- of D81 shielding the ionic interaction from solvent exposition by its hydrophobic nature. It is involved in a cation-π interaction between R155 and its left-hand side aromatic ring and in a π-π interaction with its right hand side aromatic with H57. The thiazole ring is involved in a π-π interaction with H57.

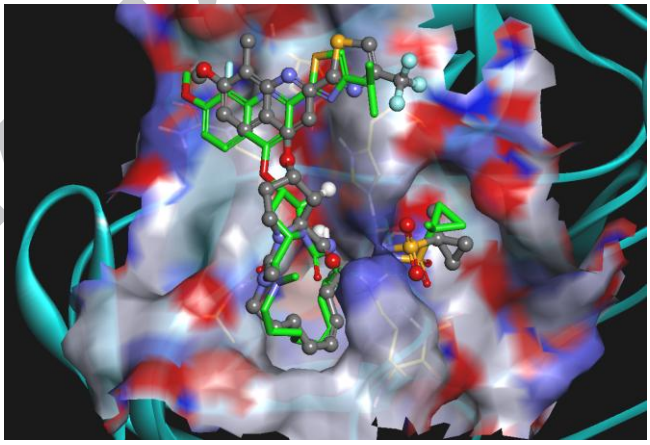

Figure 3. Overlay of compound (**7**) on the X-ray crystal structure of NS3/4A protein complex with compound (**16c**) (in green).

Modulating the substitution on the quinoline ring (Table 1) and changing the nature of the heteroaromatic ring (Table 2) at position 2 could lead to more potent compounds. Compound (**16d**) and (**16b**) with a chlorine or methyl group at position 8, while maintaining a methoxy at position 7, demonstrated good potency in the biochemical assay with 2.3 nM and 1.8 nM, respectively, and significantly improved the inhibitory activity of the replicon compared to the fluorine analogue (**16c**) by seven to over nine fold. The increasing activity observed with Br>Cl>F in both assays can be explained by a possible halogen bonding interaction with the oxygen carbonyl of V78 as studied previously.[27,28] The oxygen of the methoxy group at position 7 can be directly involved in hydrogen bonding with the arginine side chain of R155 but can also participate indirectly to the parallel displaced cation-π interaction of R155 with the quinoline by inductive effect.[29] Due to the excessive payload of the bromine atom as compared to the gain in activity observed, only the chlorine atom and methyl group were selected for optimization at position 2 of the quinoline (Table 2). The X-ray of compound (**16c**) revealed a close proximity of the 2-iso-propyl-thiazole and tyrosine (Y56). Compounds (**16p-q**) and (**16t-x**) were designed to increase interaction with the tyrosine *via* σ-π or π-π interaction, the vinyl (**16w**) and ethynyl (**16u**) and (**16v**) groups are the most active substituents with subnanomolar activity in the biochemical assay and low nanomolar activity in the cell-based

ACCEPTED MANUSCRIPT

assay. The carbonitrile group in compound (**16x**), being less electron rich than its ethynyl analogue in compound (**16t**), probably has a reduced interaction with the Y56 resulting in a lower binding affinity with an IC_{50} value of 10 nM and an EC_{50} value of 89 nM. Changing the nature of the heteroatom to a pyrazole (**16m**), a 1,2,3-triazole (**16o**), isoxazole (**16i**) or oxadiazole group (**16s**) and therefore lowering the electron density on the ring was detrimental to the activity. The 1,2,3-triazole (**16o**), isoxazole (**16i**) or oxadiazole (**16s)** groups could also affect cell permeability as seen with the fold change increase between the biochemical assay and cell-based assay (>80). It is interesting to observe that in the co-crystal structure of ligand (**16c**) with the NS3/4A protein and in other co-crystal structures generated (data not shown), the thiazole ring was always orientated in such that the sulfur atom of the thiazole ring could be engaged in a stabilizing intramolecular $n_0 \rightarrow \sigma^*$ non-bonding interaction with the quinoline nitrogen. This type of interaction between sulfur and heteroatom has been previously observed and is believed to be important in stabilizing the orientation of the two ring system to one another, therefore lowering the entropic energy of the ligand and favouring the overall binding energy.[30] However in this case, the thiazole regioisomer (**16j**) is slightly more potent than (**16d**) in the enzymatic assay and equipotent in the cellular assay; this interaction does not play a significant role in the overall binding energy of the protease inhibitor. The steric isostere[31] of the isopropyl thiazole ring bearing a trifluroromethyl group (**7**) was the best compound from this series with an IC_{50} value of 0.5 nM, an EC_{50} value of 13 nM and a CC_{50} value of >75 μM.

A few compounds from this series were selected to assess their stability in different microsome species. Replacing the 2,4-disubstituted azetidine motif in the P2 region by the 3-hydroxy-pyrrolidine as a possible structural mimic was beneficial to microsomal stability with compounds (**16d**) and (**16b**) having significant lower clearance in rat, cynomolgus monkey and human liver microsomes along with a longer half life in rat liver microsomes compared to compounds (**5**) and (**6**). The clearance obtained in rat liver microsomes and rat cryopreserved hepatocytes indicated a primary oxidative metabolism process for this series as the main route of elimination rather than a conjugative process.

The clearance in human liver microsomes remained moderate for this series, but demonstrated more sensitivity in monkey liver microsomes (Table 3).

The crystal structure of compound (**16c**) was the basis for parallel research on the pipecolic series where the P2 pyrrolidine moiety was replaced with a 4-hydroxy pipecolic acid moiety (Figure 3). The pipecolic motif has been seen previously in peptidomimetic structures such as the HIV protease inhibitor, palinavir[32], which demonstrated good pharmacokinetic in the rat.[33] Modelling this substitution with the trifluoromethyl moiety on the thiazole ring demonstrated a good overall fit with the X-ray structure of compound (**16c**). The main chain and side chain hydrogen bond interactions were maintained along with the σ-π interaction between H57 and one of the pipecolic C5-hydrogen, plus the cation-π interactions of thiazole and quinoline ring with R155. Encouraged by these findings, a few analogues with the best substitution identified in the 3-hydroxy-pyrrolidine series were synthesised to validate the binding hypothesis and evaluate the potential of this new series. The pipecolic motif series yielded extremely potent compounds (**27**), (**31a**) and (**8**) with sub nanomolar activity both in the enzymatic and the cellular inhibition assays (Table 4). These results validated the modelling hypothesis and binding energies calculated of -93kcal/mol for compounds (**16c**) as compared to the more favourable binding energies calculated of -108.9kcal/mol for compounds (**8**).[34]

The best compounds in each series, compounds (**7**) and (**8**), were selected for rat PK analysis. The plasma kinetics, oral bioavailability and liver tissue distribution in male Sprague-Dawley rats were determined after a single oral (*po*) administration of 10 mg/kg of the compounds using the sodium salt of (**7**) in a VitamineE-TPGS-PEG400-buffer pH 9.25 (2.5/17.5/80%) solution or the parent compound (**8**) in VitamineE-TPGS-PEG400-buffer pH 7.4 (2.5/17.5/80%) solution as vehicle. These data were analyzed and compared to those obtained after a single intravenous (*iv*) administration of 2 mg/kg of either compound prepared under the same conditions as above. The plasma levels were determined up to 8h post-administration *iv* and up to 24h post-administration *po*. The mean maximum concentration was obtained for both compounds after 1 hour, indicating a rapid absorption (Table 5). The clearance (Cl) was lower for (**7**) compared to (**8**) and was associated with a longer mean half-life ($t_{1/2}$), yet compound (**8**) yielded better oral absorption and higher area under the curve (AUC) concentrations that translated to a higher oral bioavailability (%F).

Table 1. Optimization of the substitution on the quinoline ring

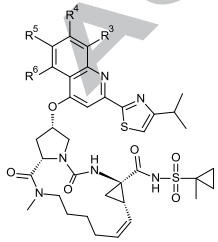

Compound	R^6	R^5	R^4	R^3	IC_{50}[a](μM)	IC_{50} SD	EC_{50}[b](μM)	EC_{50} SD	CC_{50}[c](μM)	CC_{50} SD
16a	H	H	OCH_3	H	0.0017	±0.0008	0.508	±0.027	42.70	±7.042
16b	H	H	OCH_3	CH_3	0.0018	±0.0009	0.072	±0.008	>75	-
16c	H	H	OCH_3	F	0.0035	±0.0004	0.538	±0.073	33.52	±3.048
16d	H	H	OCH_3	Cl	0.0023	±0.0008	0.056	±0.003	48.48	±7.068
16e	H	OCH_3	Cl	H	0.0086	±0.0031	0.191	±0.009	>75	-

ACCEPTED MANUSCRIPT

16f	H	H	OCH_3	Br	0.0005	±0.0003	0.029	±0.003	51.18	±8.016

[a] Biochemical FRET assay for inhibition capacity on the full length 1b Con1 HCV NS3/4A protease in triplicate.

[b] Inhibition of HCV replication Huh-7 cells containing HCV Con1 subgenomic replicon (GS4.1 cells) with a luciferase read-out in triplicate.

EC_{50} values were determined from the 50% inhibition *versus* concentration data.

[c] CC_{50}'s were calculated as the concentration that caused a 50% of cells death *versus* concentration data.

Cleavage of a synthetic peptide by purified, recombinant HCV NS3/4A protease from genotype 1b was measured with the SensoLyte™ 620 HCV Protease Assay kit from AnaSpec, Inc. (San Jose, CA). Luciferase-replicon cells (Con1, genotype 1b) were seeded onto 96-well plates, cultured for 3 days in the presence of compound and subjected to a luciferase assay. Compound cytotoxicity was measured in parallel using a colorimetric proliferation assay. IC_{50}, EC_{50} and CC_{50} values were determined from % inhibition (IC_{50} and EC_{50}) or % cytotoxicity (CC_{50}) *versus* concentration data using a sigmoidal non-linear regression analysis based on four parameters.

Table 2. Changing the nature of the heteroaromatic ring at position 2 of the quinoline

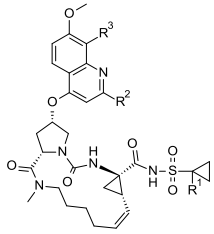

Compound	R^1	R^2	R^3	IC_{50}[a](μM)	IC_{50} SD	EC_{50}[b](μM)	EC_{50} SD	CC_{50}[c](μM)	CC_{50} SD
7	CH_3		CH_3	0.0005	±0.0002	0.013	±0.0029	>75	-
16g	H		Cl	0.0010	±0.0001	0.021	±0.0069	31.25	±2.934
16h	CH_3		Cl	0.0013	±0.0001	0.029	±0.0010	>75	-
16i	CH_3		Cl	0.0037	±0.0021	0.669	±0.0741	>75	-
16j	CH_3		Cl	0.0008	±0.0001	0.032	±0.0059	30.21	±2.865
16k	CH_3		Cl	0.0010	±0.0001	0.019	±0.0058	59.00	±4.963
16l	H		CH_3	0.0009	±0.0003	0.008	±0.0024	>75	-
16m	CH_3		CH_3	0.0009	±0.0003	0.065	±0.0051	9.61	±1.365
16n	CH_3		Cl	0.0004	±0.0001	0.027	±0.0028	21.92	±1.927
16o	CH_3		Cl	0.0073	±0.0016	0.593	±0.1279	28.54	±0.537
16p	CH_3		CH_3	0.0064	±0.0012	0.499	±0.0577	55.80	±1.151
16q	CH_3		CH_3	0.0070	±0.0010	0.085	±0.0115	>75	-
16r	H		Cl	0.0010	±0.0001	0.022	±0.0088	>75	-
16s	H		CH_3	0.0257	±0.0063	>0.750	-	>75	-
16t	CH_3		Cl	0.0005	±0.0001	0.004	±0.0005	17.04	±6.644
16u	CH_3		CH_3	0.0009	±0.0001	0.0027	±0.0013	>75	-
16v	H		CH_3	0.0009	±0.0001	0.0028	±0.0010	14.41	±0.815
16w	CH_3		Cl	0.0008	±0.0001	0.004	±0.0008	57.12	±2.475
16x	CH_3		Cl	0.010	±0.0006	0.089	±0.0114	>75	-

[a] Biochemical FRET assay for inhibition capacity on the full length (**1b)** Con1 HCV NS3/4A protease in triplicate.

[b] Inhibition of HCV replication Huh-7 cells containing HCV Con1 subgenomic replicon (GS4.1 cells) with a luciferase read-out in triplicate

EC_{50} values were determined from the 50% inhibition *versus* concentration data

[c] CC_{50}'s were calculated as the concentration that caused a 50% of cells death *versus* concentration data

Table 3. Mean clearance (n=2) observed in different species liver microsomes and cryopreserved hepatocytes.

Compound	Rat Liver Microsomes Clint	Rat Liver Microsomes t1/2	Rat Cryopreserved Hepatocytes Clint	Human Liver Microsomes Clint	Monkey Liver Microsomes Clint

ACCEPTED MANUSCRIPT

	(µl/min/mg)	(min)	(µl/min/10^6 cells)	(µl/min/mg)	(µl/min/mg)
5	364.1	3.8	N/D	299.1	500
6	182.5	8	N/D	471.9	500
7	11.4	122	17.4	24	46.7
16b	12.6	112	12.3	9.8	37.8
16d	9.7	143	11.2	18.5	66.8
16l	23.7	59	30	27.1	39.9

N/D: not determined

Table 4. Structure activity of the pipecolic scaffold

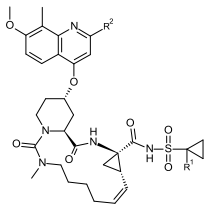

Compound	R^1	R^2	IC_{50}[a](µM)	IC_{50} SD	EC_{50}[b](µM)	EC_{50} SD	CC_{50}[c](µM)	CC_{50} SD
27	CH_3		0.0006	±0.0001	0.0002	±0.0001	>75	-
31a	H		0.0004	±0.0001	0.0009	±0.0001	>75	-
8	CH_3		0.0005	±0.0001	0.0007	±0.0002	52.78	±0.299

[a] Biochemical FRET assay for inhibition capacity on the full length (**1b)** Con1 HCV NS3/4A protease in triplicate.

[b] Inhibition of HCV replication Huh-7 cells containing HCV Con1 subgenomic replicon (GS4.1 cells) with a luciferase read-out in triplicate.

EC_{50} values were determined from the 50% inhibition *versus* concentration data.

[c] CC_{50}'s were calculated as the concentration that caused a 50% of cells death *versus* concentration data.

Table 5. male Sprague-Dawley rats mean (n=3) plasma levels and pharmacokinetic of compounds (**7**) and (**8**) analysis

Compound	Route	Dose (mg/kg)	C_{max} (ng/mL)	T_{max} (h)	AUC_t (ng.h/mL)	AUC_{inf} (ng.h/mL)	$t_{1/2}$ (h)	Cl (L/h/kg)	F (%)	Liver to plasma ratio concentration at 24h
7	*Iv*	2	2674	0.08	2537	2572	1.5	0.79	/	/
	po	10	406	1.0	2227	2377	5.2	/	18%	N/C
8	*iv*	2	2064	0.08	1751	1773	1.5	1.13	/	/
	po	10	934	1.0	3915	3966	3.6	/	45%	61.7

N/C: not calculable; Oral bioavailability (F%)

Table 6. Phamacokinetic parameters of compound (**8**) in mice and monkeys administered a single 2 mg/kg dose[a]

Species	Route	C_{max} (ng/mL)	C_{24h} (ng/mL)	T_{max} (h)	AUC[b] (ng.h/mL)	Vd (L/kg)	$t_{1/2}$ (h)	Cl (L/h/kg)	F (%)
CD-1 Mouse	*iv*	N/A	7.9±1.1	N/A	4060±356	4.4±0.3	6.3±1.0	0.48±0.04	n/a
	po	174	1.5±0.3	2	1410±86	N/A	N/C	N/A	34.7
Cynomolgus Monkey	*iv*	N/A	66±26	N/A	9580±1420	3.5±0.5	10.3±1.0	0.23±0.03	N/A
	po	1030 ±270	81±47	1.0	8920±2190	N/A	7.6±2.0	N/A	107±40

[a] vehicle: 70% PEG300/30%D5W for IV dose and PEG400 for oral dose

[b] AUC 0-24h for mouse and AUCinf for monkey

N/A: not applicable; N/C: not calculable; Oral bioavailability (F%)

ACCEPTED MANUSCRIPT

Due to the specific replication of the virus in the liver, the liver to plasma ratio was measured. While the liver level of compound (**7**) was undetectable at 24h, the liver level of compound (**8**) was detectable and the liver to plasma ratio concentration was 61.7. Based on this promising *in vivo* data, compound (**8**) was further characterised both *in vitro* and *in vivo*. The macrocycle (**8**) inhibited NS3/4A proteases from genotypes 1a, 1b, 2a and 4a (IC_{50} values from 0.8 to 1.9 nM), as well as from genotype 3a (IC_{50} value of 23 nM). Also, compound (**8**) did not inhibit nine tested cellular proteases (IC_{50} > 10 µM; data not shown), indicating high selectivity. Favourable oral bioavailability of (**8**) was observed in mouse and monkey species, with substantial plasma concentrations observed 24 h after a single 2 mg/kg oral dose (Table 6). Low clearance (less than 9% of hepatic blood flow) and relatively long plasma half-lives in both the mouse and monkey along with a high permeability (Papp=$1.8x10^{-6}$ cm/s) and a low efflux (ER=2.7) in Caco-2 cell monolayers. The selected compound was not cytotoxic to fresh mouse, rat, monkey and human hepatocytes, with CC_{50} values > 10 µM. Compound (**8**) showed no significant inhibition of human CYP450 1A2, 2B6, 2C9, 2D6, 3A4 or human UGT1A1 ($IC_{50} \geq 10$ µM). Additionally, the cardiac hERG potassium channel current in HEK293 cells was not affect by (**8**). At single oral doses up to 250 mg/kg, compound (**8**) had no effect on the cardiovascular and respiratory systems of monkeys or on the central nervous system, renal function or gastrointestinal motility of mice. (**8**) demonstrated no genotoxicity in the bacterial mutation, lymphocyte chromosomal aberration and mouse micronucleus tests. In 4-week GLP toxicology studies in mice and monkeys, the compound was well tolerated and all in-life and post-mortem parameters were generally unremarkable at oral doses up to 250 mg/kg/day. Those data supported the potential for once-daily dosing in patients.

Investigation of two series of P2 analogues that mimic the β-strand using 4-hydroxy-2-pyrrolidine acid and 4-hydroxy pipecolic acid moieties led to the discovery of potent inhibitors with improved metabolic stability compared to the 2,4-disubsituted azetidine series. X-ray co-crystal structures of the protein helped us to model the key interactions of the inhibitor and to rationalize the design of 4-hydroxy pipecolic acid series. This series with excellent potency, multi-genotypic activity in addition to good pharmacokinetic profiles in rodent and non human primate led to the selection of (**8**) (IDX320) as an HCV drug candidate for clinical development.[35]

Acknowledgments

We thank Proteros Biostructure GmbH, Dr. Christine Wenzkowski and Dr. Stefan Steinbacher for X-Ray structure determination of HCV NS3/4A protease in complex with the ligand (**16c**).

Supplementary data

Supplementary data associated (detailed characterization of compound (**8**) (IDX320)) with this article can be found in the online version.

References and notes:

1. Marubashi, S.; Dono, K.; Miyamoto, A.; Takeda, Y.; Nagano, H.; Umeshita, K.; Monden, M. *J. Hepatobiliary. Pancreat. Surg.* **2006**, *13*, 382.
2. Hoofnagle, J. H.; Seeff, L. B. *N. Engl. J. Med.* **2006**, *355*, 2444.
3. Azvolinsky, A. *Nat. Biotechnol.* **2015**, *33*, 575.
4. Chary, A.; Holodniy, M. *Rev. Recent Clin. Trials* **2010**, *5*, 158.
5. Morikawa, K.; Lange, C. M.; Gouttenoire, J.; Meylan, E.; Brass, V.; Penin, F.; Moradpour, D. *J. Viral Hepat.* **2011**, *18*, 305.
6. Reiser, M.; Timm, J. *Expert Rev. Anti Infect. Ther.* **2009**, *7*, 537.
7. Chen, K. X.; Njoroge, F. G. *Curr. Opin. Investig. Drugs Lond. Engl. 2000* **2009**, *10*, 821.
8. Forestier, N.; Zeuzem, S. *Expert Opin. Pharmacother.* **2012**, *13*, 593.
9. Rizza, S. A.; Talwani, R.; Nehra, V.; Temesgen, Z. *Drugs Today* **2011**, *47*, 743.
10. For the latest update on the best practise for HCV treatment, please refer to: http://www.hcvguidelines.org.
11. Llinàs-Brunet, M.; Bailey, M. D.; Ghiro, E.; Gorys, V.; Halmos, T.; Poirier, M.; Rancourt, J.; Goudreau, N. *J. Med. Chem.* **2004**, *47*, 6584.
12. Llinàs-Brunet, M.; Bailey, M.; Fazal, G.; Goulet, S.; Halmos, T.; Laplante, S.; Maurice, R.; Poirier, M.; Poupart, M.-A.; Thibeault, D.; Wernic, D.; Lamarre, D. *Bioorg. Med. Chem. Lett.* **1998**, *8*, 1713.
13. Rancourt, J.; Cameron, D. R.; Gorys, V.; Lamarre, D.; Poirier, M.; Thibeault, D.; Llinàs-Brunet, M. *J. Med. Chem.* **2004**, *47*, 2511.
14. Tsantrizos, Y. S.; Bolger, G.; Bonneau, P.; Cameron, D. R.; Goudreau, N.; Kukolj, G.; LaPlante, S. R.; Llinàs-Brunet, M.; Nar, H.; Lamarre, D. *Angew. Chem. Int. Ed.* **2003**, *42*, 1356.
15. Hinrichsen, H.; Benhamou, Y.; Wedemeyer, H.; Reiser, M.; Sentjens, R. E.; Calleja, J. L.; Forns, X.; Erhardt, A.; Crönlein, J.; Chaves, R. L.; Yong, C.-L.; Nehmiz, G.; Steinmann, G. G. *Gastroenterology* **2004**, *127*, 1347.
16. Raboisson, P.; de Kock, H.; Rosenquist, Å.; Nilsson, M.; Salvador-Oden, L.; Lin, T.-I.; Roue, N.; Ivanov, V.; Wähling, H.; Wickström, K.; Hamelink, E.; Edlund, M.; Vrang, L.; Vendeville, S.; Van de Vreken, W.; McGowan, D.; Tahri, A.; Hu, L.; Boutton, C.; Lenz, O.; Delouvroy, F.; Pille, G.; Surleraux, D.; Wigerinck, P.; Samuelsson, B.; Simmen, K. *Bioorg. Med. Chem. Lett.* **2008**, *18*, 4853.
17. Parsy, C.; Alexandre, F.-R.; Brandt, G.; Caillet, C.; Cappelle, S.; Chaves, D.; Convard, T.; Derock, M.; Gloux, D.; Griffon, Y.; Lallos, L.; Leroy, F.; Liuzzi, M.; Loi, A.-G.; Moulat, L.; Musiu, C.; Rahali, H.; Roques, V.; Seifer, M.; Standring, D.; Surleraux, D. *Bioorg. Med. Chem. Lett.* **2014**, *24*, 4444.
18. Arumugasamy, J.; Arunachalam, K.; Bauer, D.; Becker, A.; Caillet, C. A.; Glynn, R.; Latham, G. M.; Lim, J.; Liu, J.; Mayes, B. A.; Moussa, A.; Rosinovsky, E.; Salanson, A. E.; Soret, A. F.; Stewart, A.; Wang, J.; Wu, X. *Org. Process Res. Dev.* **2013**, *17*, 811.
19. Hoveyda, A. H.; Gillingham, D. G.; Veldhuizen, J. J. V.; Kataoka, O.; Garber, S. B.; Kingsbury, J. S.; Harrity, J. P. A. *Org. Biomol. Chem.* **2004**, *2*, 8.
20. Zhao, Z.; Zhan, Z.-Y. J. *Chim. Oggi* **2006**, *24*, 8.
21. Parsy, C.; Alexandre, F.-R.; Bonnaterre, F.; Surleraux, D. WO2010090976A1 **2010**.
22. Alexandre, F.-R.; Brandt, G.; Caillet, C.; Chaves, D.; Convard, T.; Derock, M.; Gloux, D.; Griffon, Y.; Lallos, L.; Leroy, F.; Liuzzi, M.; Loi, A.-G.; Moulat, L.; Musiu, C.; Parsy, C.; Rahali, H.; Roques, V.; Seifer, M.; Standring, D.; Surleraux, D. *Bioorg. Med. Chem. Lett.*, DOI information: 10.1016/j.bmcl.2015.07.020.
23. Co-Crystallization: The NS3/4a protein was recombinantly expressed in an E. coli expression system. An apparent homogeneity of more than 95% as judged by Coomassie-stained SDS-PAGE was achieved after a purification procedure comprising affinity, ion exchange and gel filtration chromatography steps. Crystals of the HCV NS3/4A ligand complex were prepared by the method of co-crystallisation. Diffraction data of the HCV NS3/4A ligand complex containing ligand (16c) were collected at the SWISS LIGHT SOURCE (SLS, Villigen, Switzerland). The structure was solved and refined to a final resolution of 2.8 Å (PDB code: 4U01). The crystal of space group C 2221 contains nine monomers of HCV NS3/4A in the asymmetric unit. The resulting electron density shows an unambiguous binding mode for ligand 16c, including the orientation and conformation of

ACCEPTED MANUSCRIPT

the ligand. The ligand shows high occupancy as judged by temperature factors of the atomic model.
24. Marsman, A. W.; Havenith, R. W. A.; Bethke, S.; Jenneskens, L. W.; Gleiter, R.; van Lenthe, J. H.; Lutz, M.; Spek, A. L. *J. Org. Chem.* **2000**, *65*, 4584.
25. Singh, R. K.; Tiwari, M. K.; Kim, I.-W.; Chen, Z.; Lee, J.-K. *Appl. Environ. Microbiol.* **2012**, *78*, 8817.
26. Rönn, R.; Sabnis, Y. A.; Gossas, T.; Åkerblom, E.; Helena Danielson, U.; Hallberg, A.; Johansson, A. *Bioorg. Med. Chem.* **2006**, *14*, 544.
27. Lu, Y.; Shi, T.; Wang, Y.; Yang, H.; Yan, X.; Luo, X.; Jiang, H.; Zhu, W. *J. Med. Chem.* **2009**, *52*, 2854.
28. Lemke, C. T.; Goudreau, N.; Zhao, S.; Hucke, O.; Thibeault, D.; Llinàs-Brunet, M.; White, P. W. *J. Biol. Chem.* **2011**, *286*, 11434.
29. Imai, Y. N.; Inoue, Y.; Yamamoto, Y. *J. Med. Chem.* **2007**, *50*, 1189.
30. Beno, B. R.; Yeung, K.-S.; Bartberger, M. D.; Pennington, L. D.; Meanwell, N. A. *J. Med. Chem.* **2015**, *58*, 4383.
31. Smart, B. E. *J. Fluor. Chem.* **2001**, *109*, 3.
32. Beaulieu, P. L.; Wernic, D.; Abraham; Anderson, P. C.; Bogri, T.; Bousquet, Y.; Croteau, G.; Guse, I.; Lamarre, D.; Liard, F.; Paris, W.; Thibeault, D.; Pav, S.; Tong, L. *J. Med. Chem.* **1997**, *40*, 2164.
33. Liard, F.; Jaramillo, J.; Paris, W. L.; Yoakim, C. *J. Pharm. Sci.* **1998**, *87*, 782.
34. The binding energies were calculated using the Discovery Studio 4.0 suite from BIOVIA.
35. During a drug-drug interaction study of the combination of IDX184 (nucleoside polymerase inhibitor) and IDX320 (protease inhibitor) in healthy volunteers, three serious adverse events occurred. These observed serious adverse events were elevated liver function tests detected in three subjects during post exposure safety visits. The cause of these serious adverse events in the combination study of IDX184 and IDX320 was further attributed to IDX320 and the clinical development of this drug was halted.

ACCEPTED MANUSCRIPT